ARTICLE

Click-Formed Polymer Gels with Aggregation-Induced Emission and Dual Stimuli-Responsive Behaviors

Sheng-yu Shi, Guo-ying Zhang*

CAS Key Laboratory of Soft Matter Chemistry, Department of Polymer Science and Engineering, University of Science and Technology of China, Hefei 230026, China

(Dated: Received on June 11, 2020; Accepted on June 24, 2020)

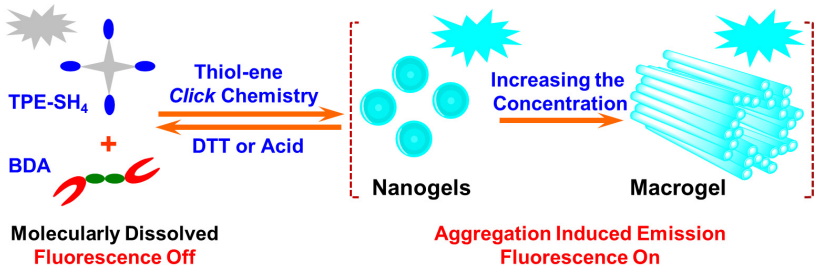

Stimuli-responsive polymer gels have recently attracted great attention due to their heat/solvent resistance, dimensional stability, and unique sensitivity to external stimuli. In this work, we synthesized thiol-functionalized tetraphenylethylene (TPE) and constructed polymer gels through thiol-ene *click* reaction. The synthetic process of the polymer gels could be monitored by fluorescence emission of TPE moieties based on aggregation-induced emission mechanism. In addition, due to the dual redox- and acid responsiveness of the polymer gels, in the presence of dithiothreitol and trifluoroacetic acid, fluorescence quenching of the polymer gels can be observed. This stimuli-responsive characteristics endows the polymer gels with potential applications in fluorescent sensing and imaging, cancer diagnosis and selfhealing materials.

Key words: Polymer gels, Thiol-ene *click* reaction, Stimuli-responsive, Aggregation-induced emission

I. INTRODUCTION

Polymer gels can be classified into two categories according to the crosslinking strategy, namely physical and chemical gels. The former can be obtained by taking advantage of non-covalent interactions, such as hydrophobic interaction, π-π stacking, multiple hydrogen bonding, metal-ligand interaction, and host-guest recognition [1−3]; while the latter are based on covalent bonds and usually formed by introduction of crosslinkers. In recent years, with the blossom of researches on reponsive polymers, plenty of stimuli-reponsive polymer gels have been developed and applied into various fields [1, 4], including but not limited to drug and gene delivery [5, 6], sensing and imaging [7−9], functional membranes [10], and intelligence device [11, 12], owing to their reponsiveness to external stimuli such as temperature, pH, solvent composition, and electric/magnetic fields. Due to the relatively higher bond energy of covalent bonds compared with those physical interactions, chemical gels always show long-lasting structural and mechanical stabilities, but less stimuli-responsive behaviors [13, 14]. Therefore, it is very fascinating to construct stimuli-responsive gel networks by simple and accessible chemical crosslinking methods, especially those with mutiple stimuli-reponsiveness thus endowing them with potential applications under complicated circumstances. In addition, integrating other functions into the polymer gels, such as fluorescence emission property, will inevitably bring them additional advantages and make them more promising for imaging and sensing applications.

*Author to whom correspondence should be addressed. E-mail: gyzhang@ustc.edu.cn

 ©2021 Chinese Physical Society

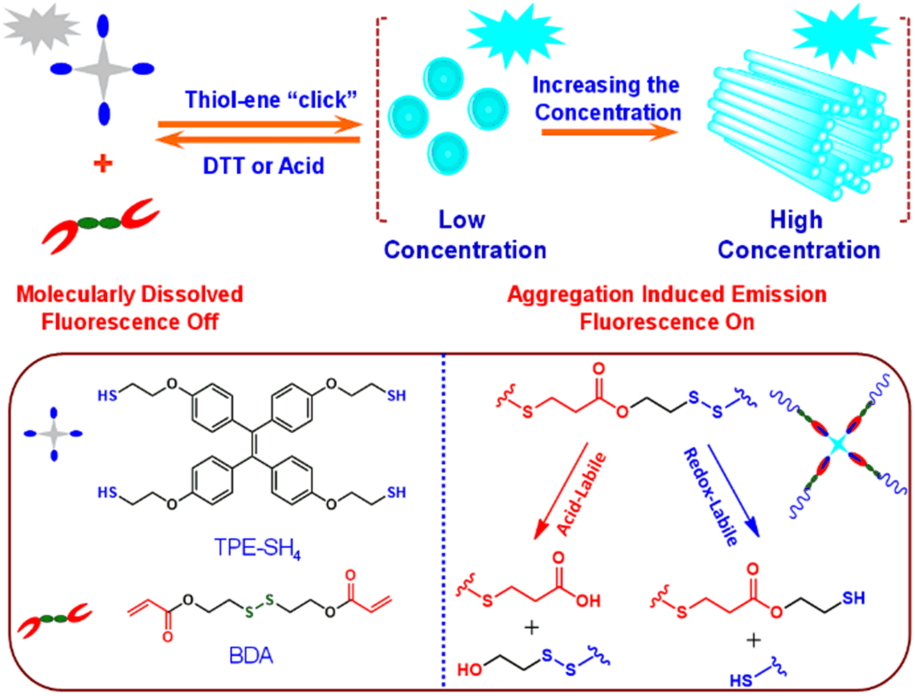

Scheme 1. Schematic illustration of the fabrication of nanogels and macrogels bearing acid- and redox-switchable aggregation induced emission characteristics from TPE-SH_4 and BDA via thiol-ene *click* reaction.

In order to construct the above-mentioned polymer gels, the choices of highly efficient reaction and appropriate components with high reactivity and unique stimuli-responsiveness are of great importance [15, 16]. Being characterized by rapid reaction speed, high regioselectivity and excellent yield under mild conditions, *click* chemistry provide a powerful strategy for the crosslinking reaction. Various kinds of *click* reactions have been applied to the preparation of polymer gels, including traditional azide-alkynes [17−19], Diels-Alder reaction, Michael addition reaction [20−22], thiol-ene and oxime reaction [23−30]. As for the highly reactive functional groups, the thiol group is considered to be one of the most promising candidates. On the other hand, in order to obtain unique stimuli-responsiveness, it is obviously advantageous to introduce some weak bonds that can be broken or cleaved under certain specific conditions. With these in mind, due to pathological environments (such as high thiol concentration and low pH), we tried to construct polymer gel networks with unique redox- and acid-responsive characteristics via thiol-ene *click* chemistry [24, 31−34]. Moreover, considering the fixation of the reactive components and the formation of insoluble gels after the covalent crosslinking reaction, tetraphenylethylene (TPE) moieties were chosen as the main structural units for the preparation of polymer gels [35−37], which were non-fluorescent when molecularly dissolved, but became highly emissive in aggregated state due to the restriction of intramolecular rotations [38−42]. Therefore, in this work, based on the aggregation-induced emission (AIE) property of TPE moieties, the preparation of polymer gels, as well as its stimuli-responsive disintegration, can be monitored by the change in the fluorescence emission intensity of TPE moieties (Scheme 1).

II. EXPERIMENTS

A. Materials

Dithiothreitol (DTT, >99.0%, Sigma-Aldrich), bis(2-hydroxyethyl) disulfide (∼90%, Fluka) and potassium thioacetate (KSAc, 99%, Acros) were used as received. 4,4′-Dihydroxybenzophenone, titanium(IV) chloride ($TiCl_4$), zinc powder (Zn), potassium carbonate (K_2CO_3), pyridine, trifluoroacetic acid (TFA), and Sodium sulfate (Na_2SO_4) (Sinopharm Chemical Reagent Co.) were used as received. Tetrahydrofuran (THF) was purified by distillation from sodium under nitrogen prior to use. 1,2-Dibromoethane and triethylamine (TEA) were dried

DOI:10.1063/1674-0068/cjcp2006090 ©2021 Chinese Physical Society

over CaH_2 and distilled just prior to use. Acetone, *N*,*N*-dimethylformamide (DMF), dimethylsulfoxide (DMSO), dichloromethane (CH_2Cl_2) (Sinopharm Chemical Reagent Co.) and all the other solvents were used as received. 1,1,2,2-Tetrakis[4-(2-bromoethoxy)phenyl]ethene (TPE-Br_4), and the two redox-responsive crosslinkers, bis(2-acryloyloxyethyl) disulfide (BDA) and *N*,*N*′-bis(acryloyl) cystamine (BAC), were prepared according to the previously published procedures [43−45], and the chemical structures of BDA and BAC were evidenced by ^{1}H NMR analysis (Scheme S1 and FIG. S1 in supplementary materials).

B. Synthesis of TPE-SAc$_4$ and TPE-SH$_4$

General protocols for synthesis of TPE-SH_4 and its precursor, TPE-SAc_4, are as follows (Scheme S1 in supplementary materials).

TPE-Br_4 (2.06 g, 2.5 mmol, 1.0 equiv.) was dissolved in DMF (20 mL). A DMF solution (10 mL) of KSAc (0.428 g, 3.75 mmol, 1.5 equiv.) was then added dropwise. The reaction was stirred at room temperature and monitored by TLC (SiO_2, CH_2Cl_2 as the eluent). After 4 h, the reaction was completed and the solvent was removed under reduced pressure. The residue was dissolved in CH_2Cl_2 (30 mL) and washed with saturated NH_4Cl for three times. The organic layers were collected and the H_2O layer was extracted once more with CH_2Cl_2. The collected CH_2Cl_2 layers were washed with HCl (1 mol/L) and brine, dried over Na_2SO_4 and concentrated under reduced pressure. The crude product was then purified by flash column chromatography (SiO_2, CH_2Cl_2) and dried in a vacuum oven overnight at room temperature to give TPE-SAc_4 (1.61 g, 80%) as a white solid. ^{1}H NMR ($CDCl_3$, δ/ppm, TMS, FIG. S2 in supplementary materials): 6.90 (8H, protons of phenyl), 6.61 (8H, protons of phenyl, 4.03 (8H, -O-CH_2-CH_2-S-), 3.20 (8H,-O-CH_2-CH_2-S-), 2.38 (12H, CH_3CO-S-).

TPE-SAc_4 (0.805 g, 1 mmol) was dissolved in dry THF. Hydrazine monohydrate (250.3 mg, 5 mmol, 5.0 equiv.) in dry THF (10 mL) was then added dropwise. The solution was then refluxed overnight. After the reaction, THF was removed under vacuum. Brine (50 mL) was then added and the mixture was extracted with CH_2Cl_2 for three times. The collected organic phase was washed with brine, dried over Na_2SO_4 and the solvent was removed under vacuum. The crude product was further purified by flash column chromatography (SiO_2, CH_2Cl_2) and then dried in a vacuum oven overnight at room temperature to give TPE-SH_4 (318 mg, 50%) as a white solid. ^{1}H NMR ($CDCl_3$, δ/ppm, TMS, FIG. S2 in supplementary materials): 6.93 (8H, protons of phenyl), 6.67 (8H, protons of phenyl), 4.08 (8H, -O-CH_2-CH_2-S-), 2.88 (8H, -O-CH_2-CH_2-SH).

C. Characterization

All ^{1}H NMR spectra were recorded on a Bruker AV300 NMR spectrometer (resonance frequency of 300 MHz for ^{1}H) operated in the Fourier transform mode. $CDCl_3$ was used as the solvent. Fluorescent images were recorded on a LEICA SP2 confocal microscope. Transmission electron microscopy (TEM) observations were conducted on a JEOL 2010 electron microscope at an acceleration voltage of 200 kV. Field-emission scanning electron microscope (FE-SEM) analysis was performed on a high resolution JEOL JSM-6700 field-emission scanning electron microscopy. Fluorescence spectra were recorded on F-4600 (Hitachi) spectrofluorometer. The slit widths were set at 5 nm both for excitation and emission, and the excitation wavelength was fixed at 390 nm. Confocal laser scanning microscopy (CLSM) images were acquired using a Leica TCS SP5 microscope. Dynamic light scattering (DLS) experiments were conducted on a Malvern Zetasizer Nano ZS Instrument. Atomic force microscopy (AFM) measurements were performed on a Digital Instrument Multimode Nanoscope IIID operating in the tapping mode under ambient conditions. Silicon cantilever (RFESP) with resonance frequency of ∼80 kHz and spring constant of ∼3 N/m was used. The setpoint amplitude ratio was maintained at 0.7 to minimize sample deformation induced by the tip. The sample was prepared by dip coating the mixed solution after incubation for 30 min of TPE-SH_4 (6.25 mmol/L) and BDA (12.5 mmol/L) in DMSO onto freshly cleaved mica surfaces. Non-oscillatory rheological measurement was performed using the TA AR-G2 rheometer (parallel plate, 20 mm diameter) at (25±1) °C. The measuring process was controlled via PC through an interface whereby the shear stress at different shear rates was automatically recorded.

III. RESULTS AND DISCUSSION

The crosslinking reaction between TPE-SH_4 and BDA was carried out in DMSO and the change in

DOI:10.1063/1674-0068/cjcp2006090 ©2021 Chinese Physical Society

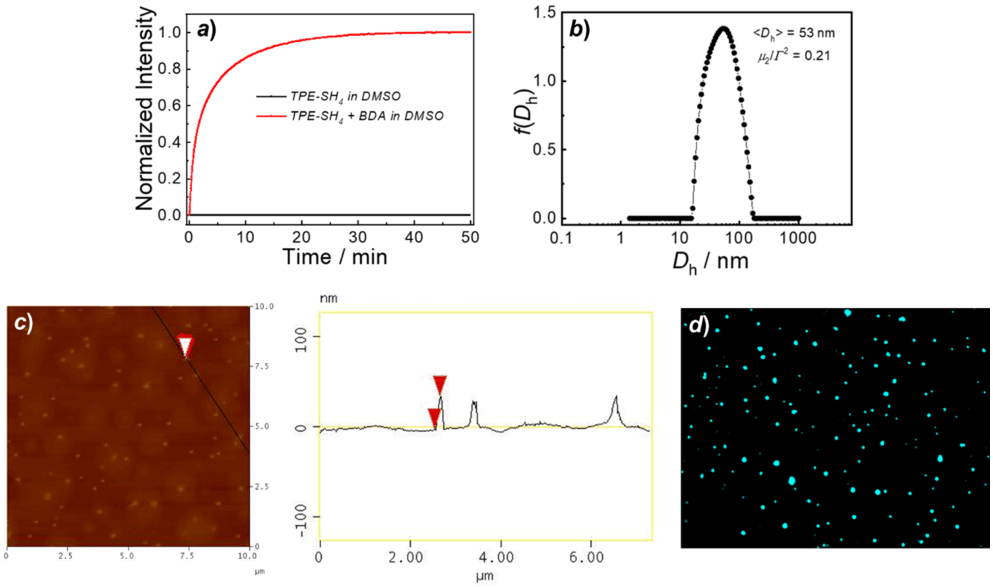

FIG. 1 (a) Normalized time-dependent fluorescence emission intensities (λ_{ex}=390 nm, λ_{em}=478 nm; slit width: Ex. 5 nm, Em. 5 nm) recorded for TPE-SH_4 (black line), and the reaction mixture of TPE-SH_4 and BDA in DMSO (red line), respectively. (b) Hydrodynamic diameter distribution, $f(D_h)$. (c) Typical AFM height images recorded for nanogels fabricated from TPE-SH_4 and BDA. (d) Confocal fluorescence images recorded for the reaction mixture of TPE-SH_4 and BDA in DMSO. For the crosslinking reaction, the original concentration of TPE-SH_4 and BDA in DMSO were fixed to be 6.25 and 12.5 mmol/L respectively; the DLS results, AFM and confocal images of the nanogels were obtained after reaction for 30 min at 25 °C.

the fluorescence emission typical of TPE moieties was recorded for the reaction solution. As shown in FIG. 1, TPE-SH_4 can be molecularly dissolved in DMSO without fluorescence emission with a concentration of 6.25 mmol/L. However, when BDA (12.5 mmol/L) was added into the solution, the fluorescence intensity of TPE increased dramatically and then stabilized after about 20 min, and the cumulative increase in fluorescence intensity was calculated to be approximately 1116 times (FIG. 1(a)). Obviously, the fluorescence intensity enhancement of TPE should be ascribed to the highly efficient thiol-ene *click* reaction between the thiol groups of TPE-SH_4 and the activated double bond of BDA, which leads to the formation of the crosslinked network. As a result, the movement and rotation of the phenyl rings in TPE were restricted, so as the polymerization proceeded, the fluorescence intensity gradually increased. To establish the above conclusion, it is necessary to rule out the possibility of the crosslinking between TPE-SH_4 molecules themselves as a result of oxidation of the thiol groups by DMSO to form disulfide linkages. We monitored the fluorescence change of TPE-SH_4 in DMSO without BDA and found that the fluorescence intensity kept almost invariant during the same time range (FIG. 1(a)), which indicates clearly that the coupling reaction between TPE-SH_4 via the oxidation of the thiol groups is negligible in this system compared to the crosslinking via thiol-ene *click* reaction.

Along with the observation on the change of fluorescence emission, dynamic laser light scattering (DLS) measurements were also performed on the mixture solution of TPE-SH_4 (6.25 mmol/L) and BDA (12.5 mmol/L). It was found that after 30 min of reaction, nanoaggregates with an intensity-average hydrodynamic diameter, $\langle D_h \rangle$, of ~53 nm can be detected, and the corresponding size polydispersity (μ_2/Γ^2) was ~0.21 (FIG. 1(b)). In the AFM image, the nanoaggregates exhibited as spherical nanoparticles, and the particle size was about 36.2 nm, as shown in the AFM height image (FIG. 1(c)). In view of that the AFM images were taken in dry state and the crosslinked nanoparticles may collapse, the difference in the particle size obtained from DLS and AFM was quite reasonable and acceptable. Therefore, it can be concluded that crosslinked nanoparticles, *i.e.* nanogels, were successfully prepared via thiol-ene *click* reaction between TPE-SH_4 and BDA. Moreover, the formation of the nanogels can be further evidenced by confocal microscopy based on AIE mechanism. In the absence of BDA, no fluores-

DOI:10.1063/1674-0068/cjcp2006090 ©2021 Chinese Physical Society

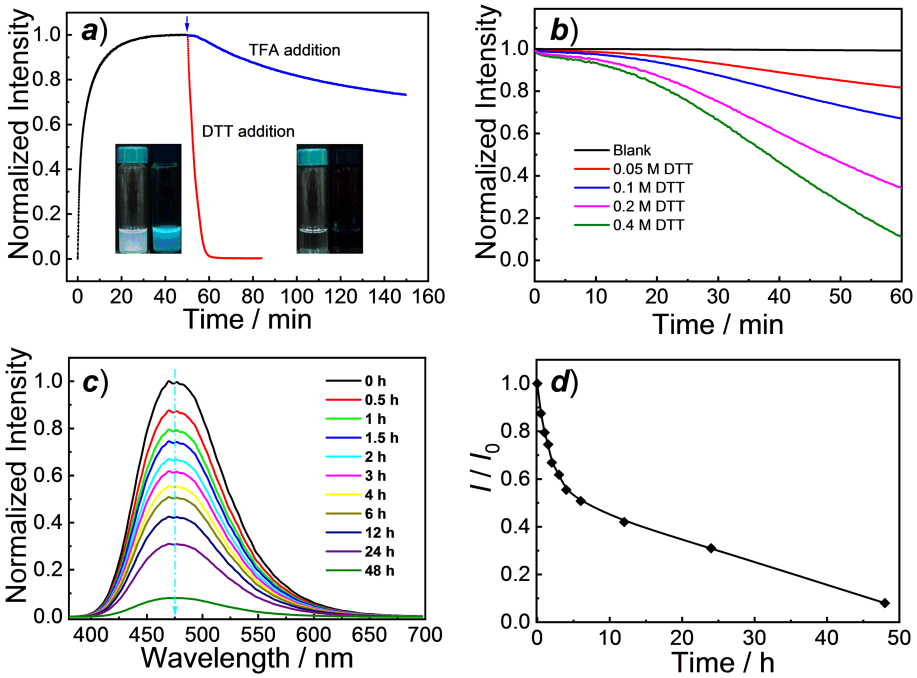

FIG. 2 (a) Time-dependent normalized fluorescence intensities (λ_{ex}=390 nm, λ_{em}=478 nm, slit width: Ex. 5 nm, Em. 5 nm) recorded for the TPE-SH_4 solution in DMSO (6.25 mmol/L) upon successive addition of BDA (12.5 mmol/L, black line) and trifluoroacetic acid (TFA, 25 mmol/L; blue line) or dithiothreitol (DTT, 0.5 mol/L; red line), respectively. (b) Time-dependent changes in the normalized fluorescence intensity (λ_{ex}=390 nm, λ_{em}=478 nm; slit width: Ex. 5 nm, Em. 5 nm) of nanogel system in DMSO upon addition of varying amount of DTT. (c) Fluorescence spectra and (d) time-dependent normalized fluorescence intensity change recorded for the nanogels in DMSO upon addition of 25 mmol/L TFA.

cence emission can be observed for the solution of TPE-SH_4, while after the crosslinking reaction with BDA, nanoparticles with typical cyan fluorescence of aggregated TPE moieties can be explicitly distinguished in the confocal fluorescence image (FIG. 1(d)).

In addition to the fluorescence "switch on" behavior, another crucial characteristic in these nanogels is the intriguing chemical structure of the crosslinked network. Taking into account the presence of the disulfide bonds and the β-thiopropionate linkers resulting from thiol-ene *click* reaction between thiol groups and acrylates that endow the system with redox- and acid-responsiveness, it can be deduced that if introducing acid or thiol-containing compounds into the crosslinked system, the nanogels will be disintegrated due to the breakage of the β-thiopropionate moieties or the disulfide bonds, respectively (Scheme 1). As a result, the mobility and the intramolecular motions of TPE moieties will recover, thus leading to decreased fluorescence emission.

To testify the above speculation, a series of fluorescence measurements upon addition of varying amount of dithiothreitol (DTT) or trifluoroacetic acid (TFA) were conducted. Firstly, the redox-responsive performance of the nanogels was verified. After BDA was introduced into the DMSO solution of TPE-SH_4 and incubated together for 50 min, during which time the crosslinked nanogels were formed, high concentration DTT (0.5 mol/L) was added. The fluorescent emission intensity of the system decreased dramatically and no fluorescence can be detected after 10 min, accompanied by the macroscopic color transition from milky to transparent. And the decrease in fluorescence emission can also be facilely observed by naked eye under UV 365 nm irradiation (FIG. 2(a)). While in contrast, the fluorescence emission of the nanogel system was rather stable in the absence of DTT (FIG. 2(b)), which suggests that the decreased fluorescence intensity should be attributed to the disassociation of the nanogels caused by the cleavage of the disulfide bonds upon addition of DTT. Furthermore, considering the potential application of the nanogels, DTT concentration was gradually reduced and the similar fluorescence changes can be observed within the same time-range. Typically, even when the DTT concentration was as low as 50 mmol/L, ~18.3% fluorescence intensity decrease

DOI:10.1063/1674-0068/cjcp2006090 ©2021 Chinese Physical Society

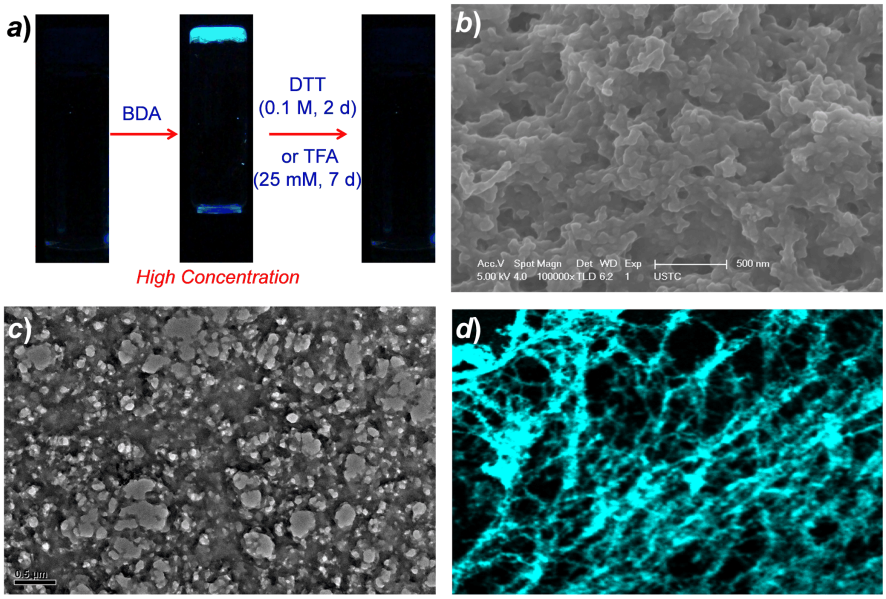

FIG. 3 (a) Macroscopic images taken under UV 365 irradiation for the macrogel fabricated from TPE-SH_4 and BDA in DMSO before and after the addition of TFA or DTT. (b) Typical SEM, (c) TEM, and (d) confocal fluorescence image recorded for the macrogel respectively. For the preparation of the macrogel, the original concentrations of TPE-SH_4 and BDA in DMSO were fixed to be as high as 50 and 100 mmol/L respectively.

can be achieved within the first 60 min, and higher DTT concentration led to more prominent fluorescence quenching (FIG. 2(b)).

Secondly, the acid-sensitive property of the nanogels originated from the β-thiopropionate linkers that can be selectively cleaved under mild acidic conditions was examined. Following the similar protocol, TFA (25 mmol/L) was added to the nanogel system. As expected, ∼27% fluorescence emission decrease can be achieved within the first 100 min. Further extending the monitoring time to 48 h, the fluorescence emission of the nanogel system almost completely disappeared and only ∼8% fluorescence residual can be detected (FIG. 2 (c) and d). To deeply investigate the intrinsic nature of the acid-responsiveness of the nanogel system, as a control, we synthesized another disulfide bond-containing bisacrylamide derivative, N,N'-bis(acryloyl) cystamine (BAC, Scheme S1 in supplementary materials), by amidation of cystamine dihydrochloride in the presence of acryloyl chloride (Scheme S1 in supplementary materials). The chemical structure of BAC was confirmed by the ^{1}H NMR experiment result (FIG. S2 in supplementary materials). It was found that crosslinked nanoaggregates can also be formed in the DMSO solution of TPE-SH_4 upon addition of BAC via thiol-ene *click* reaction. However, the crosslinked aggregates seemed extremely stable and exhibited inappreciable fluorescence intensity change even being treated with TFA for 48 h (FIG. S3 in supplementary materials), which revealed the stability of β-thiopropionamide group in acidic environments and, in turn, demonstrated that the acid-responsive behavior of the nanogels obtained from TPE-SH_4 and BDA should be ascribed to the presence of the β-thiopropionate linkers in the crosslinked network.

Based on the above experimental results, we now can safely conclude that a novel nanogel platform with dual redox- and acid-responsive characteristics has been successfully fabricated through highly efficient thiol-ene *click* chemistry, and at the same time, AIE mechanism was integrated into the system to facilely monitor the formation and stimuli-responsive disintegration of the nanogels. In the next step, in order to extensively and thoroughly explore the application of thiol-ene *click* chemistry in the preparation of polymer networks, the crosslinking of TPE-SH_4 and BDA was performed at a relatively high concentration. The photo recorded in the vial inversion test evidently certified the fromation of crosslinked networks, *i.e.* macrogel, from TPE-SH_4 and BDA with the concentration as high as 50 mmol/L and 100 mmol/L, respectively (FIG. 3(a)). Oscillatory shear experiment on the macrogel revealed an elastic performance (FIG. S4 in supplementary materials), the storage modulus (G') is higher than the loss modulus (G'') over the entire frequency range, giving a G' value

DOI:10.1063/1674-0068/cjcp2006090 ©2021 Chinese Physical Society

as high as $\sim 10^3$ Pa at the frequency of 100 rad/s and a maximum value of G'' at 0.02 rad/s. Besides, the three-dimensional structure of the macrogel was further observed by SEM, TEM, and confocal fluorescence microscopy, which manifested to be fibrously crosslinked (FIG. 3(b−d)).

Finally, the redox- and acid-responsiveness of the macrogel were also investigated upon addition of DTT or TFA. It was found that the three-dimensional crosslinked networks could also be degraded in the presence of DTT or TFA, while the degradation time is significantly longer than that of nanogels fabricated from TPE-SH_4 and BDA at the relatively low concentration. More specifically, for redox-responsiveness, the degradation of the three-dimensional macrogel can be completed within 2 days in the presence of 0.1 mol/L DTT. However, as for the acid-reponsiveness, prominent disintegration only can be accomplished after 7 days upon addition of 25 mmol/L TFA (FIG. 3(a)). The apparently increased degradation time should be ascribed to the complex three-dimensional networks formed at high concentration.

IV. CONCLUSION

In summary, we herein report a robust three-dimensional network fabricated from thiol-ene *click* chemistry with redox- and acid-responsive behavior and switchable fluorescence emission. Thiol group-terminated TPE (TPE-SH_4) with AIE character and bisacrylate derivative bearing disulfide bonds (BDA) were synthesized. In organic solvent (*i.e.*, DMSO), nanogel and macrogel with "turn on" fluorescence behavior could be facilely achieved within 30 min from TPE-SH_4 and BDA at low and high concentration, respectively. Due to the presence of redox-responsive disulfide bonds and the acid-sensitive β-thiopropionate linkers, the gels can be selectively disintegrated upon addition of DTT and TFA, respectively. Moreover, the formation and the stimuli-responsive degradation processes can be recognized by the change in the fluorescence emission intensity of TPE moieties based on AIE mechanism.

Supplementary materials: The synthetic route and ^{1}H NMR spectra of TPE-SH_4 and two redox-responsive crosslinkers, as well as the oscillatory shear experiment results of the formed macrogel are given.

V. ACKNOWLEDGMENTS

This work was supported by the National Natural Science Foundation of China (No.51773190 and No.51973206).

[1] X. F Ji, Y. Yao, J. Y. Li, X. Z. Yan, and F. H. Huang, J. Am. Chem. Soc. **135**, 74 (2013).
[2] S. Seiffert and J. Sprakel, Chem. Soc. Rev. **41**, 909 (2012).
[3] L. Wang, L. Cheng, G. Li, K. Liu, Z. Zhang, P. Li, S. Dong, W. Yu, F. Huang, and X. Yan, J. Am. Chem. Soc. **142**, 2051 (2020).
[4] T. Kureha, D. Aoki, S. Hiroshige, K. Iijima, D. Aoki, T. Takata, D. Suzuki, Angew. Chem. Int. Ed. **56**, 15393 (2017).
[5] J. H. Ryu, R. T. Chacko, S. Jiwpanich, S. Bickerton, R. P. Babu, and S. Thayumanavan, J. Am. Chem. Soc. **132**, 17227 (2010).
[6] K. N. Zhu, Z. Y. Deng, G. H Liu, J. M. Hu, and S. Y. Liu, Macromolecules **50**, 1113 (2017).
[7] S. Schmidt, T. J. Paul, and A. K. Strzelczyk, Macromol. Chem. Phys. **220**, 1900323 (2019).
[8] A. Hussain, A. T. S. Semeano, S. Palma, A. S. Pina, J. Almeida, B. F. Medrado, A. Padua, A. L. Carvalho, M. Dionisio, R. W. C. Li, H. Gamboa, R. V. Ulijn, J. Gruber, and A. C. A. Roque, Adv. Funct. Mater. **27**, 1700803 (2017).
[9] A. Vidyasagar and K. M. Sureshan, Angew. Chem. Int. Ed. **54**, 12078 (2015).
[10] J. Xue, L. Liu, J. Liao, Y. Shen, and N. Li, J. Mater. Chem. A **6**, 11317 (2018).
[11] J. Liu, C. S. Y. Tan, Z. Yu, N. Li, C. Abell, and O. A. Scherman, Adv. Mater. **29**, 1605325 (2017).
[12] J. H. Choi, G. K. Pande, Y. R. Lee, and J. S. Park, Polymer **194**, 122402 (2020).
[13] C. Chen, J. Tan, M. C. Hsieh, T. Pan, J. T. Goodwin, A. K. Mehta, M. A. Grover, and D. G. Lynn, Nat. Chem. **9**, 799 (2017).
[14] T. Gilbert, N. M. B. Smeets, and T. Hoare, ACS Macro Lett. **4**, 1104 (2015).
[15] J. M. Hu and S. Y. Liu, Accounts Chem. Res. **47**, 2084 (2014).
[16] J. M. Hu and S. Y. Liu, Sci. China Chem. **60**, 1153 (2017).
[17] V. Crescenzi, L. Cornelio, C. Di Meo, S. Nardecchia, R. Lamanna, Biomacromolecules **8**, 1844 (2007).
[18] C. A. DeForest, B. D. Polizzotti, and K. S. Anseth, Nat. Mater. **8**, 659 (2009).
[19] M. Malkoch, R. Vestberg, N. Gupta, L. Mespouille, P. Dubois, A.F. Mason, J. L. Hedrick, Q. Liao, C. W. Frank, K. Kingsbury, and C. J. Hawker, Chem. Commun. **26**, 2774 (2006).

DOI:10.1063/1674-0068/cjcp2006090 ©2021 Chinese Physical Society

[20] P. M. Kharkar, A. M. Kloxin, and K. L. Kiick, J. Mater. Chem. B **2**, 5511 (2014).
[21] R. J. Pounder, M. J. Stanford, P. Brooks, S. P. Richards, and A. P. Dove, Chem. Commun. **41**, 5158 (2008).
[22] D. P. Nair, M. Podgórski, S. Chatani, T. Gong, W. Xi, C. R. Fenoli, and C. N. Bowman, Chem. Mater. **26**, 724 (2013).
[23] R. Mahou and C. Wandrey, Macromolecules **43**, 1371 (2010).
[24] H. Shih and C. C. Lin, Biomacromolecules **13**, 2003 (2012).
[25] M. S. Rehmann, A. C. Garibian, and A. M. Kloxin, Macromol. Symp. **329**, 58 (2013).
[26] H. Shih and C. C. Lin, Biomacromolecules **16**, 1915 (2015).
[27] B. Yan, H. Zhou, J. Lai, Z. Wang, C. Luo, H. Liu, X. Jin, A. Ma, and W. Chen, Polym. Bull. **76**, 6049 (2019).
[28] S. Park, B. Jeong, D. A. Lim, C. H. Lee, K. H. Ahn, J. H. Lee, and D. W. Kim, ACS Appl. Mater. Inter. **12**, 19553 (2020).
[29] Q. T. Phan, M. P. Patil, T. T. K. Tu, G. D. Kim, and K. T. Lim, React. Funct. Polym. **147**, 104463 (2020).
[30] S. A. Stewart, M. B. Coulson, C. Zhou, N. A. D. Burke, and H. D. H. Stover, Soft Matter **14**, 8317 (2018).
[31] A. B. Lowe, Polym. Chem. **1**, 17 (2010).
[32] N. Naga, K. Moriyama, and H. Furukawa, J. Polym. Sci. Pol. Chem. **55**, 3749 (2017).
[33] K. Peng, J. Sun, Y. Wang, Y. Li, B. Zhang, and B. Wang, J. Appl. Polym. Sci. **131**, 40930 (2014).
[34] Q. Peng, C. Hu, J. Cheng, Z. Zhong, and R. Zhuo, Bioconjugate Chem. **20**, 340 (2009).
[35] L. Shao, J. Sun, B. Hua, and F. Huang, Chem. Commun. **54**, 4866 (2018).
[36] C. W. Zhang, B. Ou, S. T. Jiang, G. Q. Yin, L. J. Chen, L. Xu, X. Li, and H. B. Yang, Polym. Chem. **9**, 2021 (2018).
[37] Y. Y. Chen, G. F. Gong, Y. Q. Fan, Q. Zhou, Q.P. Zhang, H. Yao, Y. M. Zhang, T. B. Wei, and Q. Lin, Soft Matter **15**, 6878 (2019).
[38] X. Gao, X. Shu, Y. Song, J. Cao, M. Gao, F. Wang, Y. Wang, J. Z. Sun, J. Liu, and B. Z. Tang, Chem. Commun. **55**, 8321 (2019).
[39] J. Mei, Y. Hong, J. W. Lam, A. Qin, Y. Tang, and B. Z. Tang, Adv. Mater. **26**, 5429 (2014).
[40] J. Mei, N. L. Leung, R. T. Kwok, J. W. Lam, and B. Z. Tang, Chem. Rev. **115**, 11718 (2015).
[41] B. Z. Tang, Z. Zhao, H. Zhang, and J. W. Y. Lam, Angew. Chem. Int. Ed. **59**, 9888 (2020).
[42] D. Wang, M. M. S Lee, W. H Xu, G. G. Shan, X.Y. Zheng, R. T. K. Kwok, J. W. Y. Lam, X. L. Hu, B. Z. Tang, and Z. Zhao, Angew. Chem. Int. Ed. **58**, 5628 (2019).
[43] Y. F. Dong, W. L. Wang, C. W. Zhong, J. B. Shi, B. Tong, X. Feng, J. G. Zhi, and Y. P. Dong, Tetrahedron Lett. **55**, 1496 (2014).
[44] (a) T. Y. Zhao, H. Zhang, B. Newland, A. Aied, D. Z. Zhou, and W. X. Wang, J. Mater. Chem. **22**, 8622 (2012).
(b) T. Y. Zhao, H. Zhang, B. Newland, A. Aied, D. Z. Zhou, and W. X. Wang, Angew. Chem. Int. Ed. **53**, 6095 (2014).
[45] M. Beija, Y. Li, A. B. Lowe, T. P. Davis, and C. Boyer, Eur. Polym. J. **49**, 3060 (2013).

DOI:10.1063/1674-0068/cjcp2006090 ©2021 Chinese Physical Society